Journal of Photochemistry and Photobiology A: Chemistry 217 (2011) 333–340

Contents lists available at ScienceDirect

Journal of Photochemistry and Photobiology A: Chemistry

journal homepage: www.elsevier.com/locate/jphotochem

Analysis of photoinduced electron transfer in flavodoxin

Kiattisak Lugsanangarm[a], Somsak Pianwanit[a], Sirirat Kokpol[a,b,*], Fumio Tanaka[c,**], Haik Chosrowjan[d], Seiji Taniguchi[d], Noboru Mataga[d]

[a] Department of Chemistry, Faculty of Science, Chulalongkorn University, Bangkok 10330, Thailand
[b] Center of Excellence for Petroleum, Petrochemicals, and Advanced Materials, Chulalongkorn University, Bangkok 10330, Thailand
[c] Department of Biochemistry, Center for Excellence in Protein Structure and Function, Faculty of Science, Mahidol University, Bangkok 10400, Thailand
[d] Division of Laser BioScience, Institute for Laser Technology, Utsubo-Honmachi, 1-8-4, Nishiku, Osaka 550-0004, Japan

ARTICLE INFO

Article history:
Received 26 August 2010
Received in revised form 29 October 2010
Accepted 1 November 2010
Available online 10 November 2010

Keywords:
Flavodoxin
Photoinduced electron transfer
Molecular dynamic simulation
Kakitani and Mataga theory

ABSTRACT

Flavodoxin (FD) from *Desulfovibrio vulgaris*, strain Miyazaki F., is a small flavoprotein that is considered to function in the transport of electrons between proteins. The observed fluorescence dynamics of FD revealed two lifetime components, a major (0.92) component at 0.158 ps and a minor (0.08) one at longer than 500 ps. Photoinduced electron transfer (ET) from Trp59 and/or Tyr97 to the excited isoalloxazine (Iso*) in FD were analyzed with atomic coordinates determined by molecular dynamic simulations (MD), the Kakitani and Mataga ET theory and the observed fluorescence dynamics with and without the minor longer decay component. The observed fluorescence decay with its long tail was not satisfactorily reproduced by the present method. We interpreted the longer lifetime component to be free flavin mononucleotide (FMN) liberated from the protein. The ET rate was faster from Trp59 to Iso* than that from Tyr97 to Iso*, despite the fact that the donor–acceptor distance was shorter in Tyr97–Iso* (mean 0.54 nm) than in Trp59–Iso* (mean 0.64 nm), as elucidated by means of electrostatic (*ES*) energy. Interactions in the Trp59–Iso*–Tyr97 system were quantum chemically studied using the conformations extracted from 46 MD snapshots at 40 ps time intervals with a PM6 semi-empirical molecular orbital (MO) method of the conformations. Dipole moments of the systems were mostly much greater than that of Iso* alone, and its directions were from Iso* to Trp59. MO analyses revealed that charge transfer takes place mostly from Trp59 to Iso*, which is in accordance with the ET analysis. Correlations between interaction energies and charge density were also examined. Absolute value of the energy increased with amount of the charge transferred.

1. Introduction

Flavoproteins play an important role in oxidation-reduction reactions in all living organisms as mammals, plants and microorganisms [1]. Some flavoproteins function as photoreceptors [2–5]. Photoinduced electron transfer (ET) in these flavin photoreceptors is the first step of their functions. Various electron transfer theories have been modeled for bulk solutions [6–9]. However, it is not clear whether these theories are applicable to ET in proteins. It has been difficult to quantitatively analyze ET in proteins, because the microenvironment around the ET donor and acceptor are heterogeneous, and ET theories in proteins contain several unknown parameters. We have quantitatively analyzed ET in flavoproteins, from their time-resolved fluorescence and molecular dynamic simulations (MD) with an ET theory [10–13].

Flavodoxins (FD) are a group of small flavoproteins with a molecular weight of 15–23 kDa, that have been isolated from a variety of microorganisms. Flavodoxins are considered to function as electron transport proteins in various metabolic pathways [14–16]. They contain a single molecule of non covalent-bound flavin mononucleotide (FMN) as the reaction center. The FD from *Desulfobivrio vulgaris*, strain Miyazaki F., was first characterized by Kitamura et al. [17]. Revealing that the dissociation constant of FMN from FD was 0.38 nM, and its redox potentials were $E_1 = -434$ mV for the oxidized-semiquinone reaction and $E_2 = -151$ mV for the semiquinone-2-electron reduced reaction.

The three dimensional structure of FD has not been experimentally determined yet, so we obtained the potential structure of the FD by means of homology modeling method (unpublished work). According to this structure, the FD isoalloxazine ring (Iso) is sandwiched by the Tyr97 and Trp59 residue, which is reassuringly similar to that reported for the FD from *Desulfovibrio vulgaris*, Hildenborough [18].

* Corresponding author at: Department of Chemistry, Faculty of Science, Chulalongkorn University, Bangkok 10330, Thailand. Tel.: +66 2 218 7583; fax: +66 2 218 7598.
** Corresponding author. Department of Biochemistry, Center for Excellence in Protein Structure and Function, Faculty of Science, Mahidol University, Bangkok 10400, Thailand.
E-mail addresses: siriratkokpol@gmail.com (S. Kokpol), fukoh2003@yahoo.com (F. Tanaka).

1010-6030/$ – see front matter © 2010 Elsevier B.V. All rights reserved.
doi:10.1016/j.jphotochem.2010.11.001

The fluorescence dynamics of wild type (WT), Y97F (Tyr97 is replaced by Phe), W59F (Trp59 is replaced by Phe), and the double mutants W59F-Y97F (DM) were measured in the sub-picoseconds time domain by means of the fluorescence up-conversion method by Mataga et al. [19]. These ultra-short lifetimes are considered to have been induced by ET from the aromatic amino acids to the excited isoalloxazine (Iso*) [20–23]. The observed fluorescence dynamics of the WT FD contains two lifetime components, 0.158 ps (0.92) and longer than 500 ps (0.08). The longer lifetime component was interpreted as being due to FMN liberated from the FD [24,25], even though the dissociation constant is very low (0.38 nM) [17].

It is required to establish a method to analyze ET mechanism in proteins. To contribute to it, we have investigated ET mechanism in FD from the fluorescence dynamics and also charge transfer interaction in Trp59–Iso*–Tyr97 systems with a semi-empirical molecular orbital method (MO).

2. Method of analyses

2.1. Homology modeling and MD calculation

The three dimensional structure of FD has not yet been determined by X-ray diffraction method or NMR spectroscopy. Therefore, we deduced its likely structure by means of homology modeling [26] using the Modeller module of the Discovery Studio 2.0 (website, http://www.discoverystudios.com). MD calculations were performed using the Amber 10 software package [27], as described elsewhere [10–13]. In addition, a total of 5760 water molecules were added to complete the system.

2.2. ET theory

The original Marcus ET theory [6] has been modified in the various ways [7–9]. In the present analysis the Kakitani and Mataga (KM) theory [9] was used, because it has given satisfactory results for static ET analyses in several flavoproteins [24,25], and dynamic ET analyses in FMN-bp [10,11] and AppA [12,13]. The ET rate as described by KM theory [9] is expressed by Eq. (1).

$$k_{\mathrm{ET}}^{j} = \frac{\nu_0^q}{1+\exp\{\beta^q(R_j - R_0^q)\}}\sqrt{\frac{k_B T}{4\pi\lambda_S^{qj}}}\exp\left[-\frac{\{\Delta G_q^0 - e^2/\varepsilon_0 R_j + \lambda_S^{qj} + ES_j\}^2}{4\lambda_S^{qj}k_B T}\right] \quad (1)$$

where k_{ET}^{j} is the ET rate from a donor j to Iso*, and the index q denotes Trp or Tyr. ν_0^q is an adiabatic frequency, β^q ET process coefficient. R_j and R_0^q are the donor j–Iso distance and its critical distance for the ET process, respectively. R_j was expressed as a center-to-center (R_c) distance rather than an edge-to-edge distance [10–13,24,25]. The ET process is adiabatic when $R_j < R_0^q$, and non-adiabatic when $R_j > R_0^q$. The terms k_B, T and e are the Boltzmann constant, temperature and electron charge, respectively. ES_j is the electrostatic (ES) energy, which is described in Eq. (5) below.

The solvent reorganization energy (λ_S^{qj}) is [6] of the ET donor q and j, is expressed as Eq. (2).

$$\lambda_S^{qj} = e^2\left(\frac{1}{2a_{\mathrm{Iso}}} + \frac{1}{2a_q} - \frac{1}{R_j}\right)\left(\frac{1}{\varepsilon_\infty} - \frac{1}{\varepsilon_0}\right) \quad (2)$$

where a_{Iso} and a_q are the radii of Iso and Trp or Tyr when these reactants are assumed to be spherical, and ε_∞ and ε_0 are the optical and static dielectric constants, respectively. The optical dielectric constant used in this study was 2.0. The radii of Iso, Trp and Tyr were determined as before [10–13,24,25], with the value of a_{Iso}, a_{Trp} and a_{Tyr} being 0.224, 0.196 and 0.173 nm, respectively.

The standard free energy change was expressed with the ionization potential of the ET donor, E_{IP}^q, as shown in Eq. (3).

$$\Delta G_q^0 = E_{\mathrm{IP}}^q - G_{\mathrm{Iso}}^0 \quad (3)$$

G_{Iso}^0 is the standard Gibbs energy related to electron affinity of Iso*. The values of E_{IP}^q for Trp and Tyr were 7.2 eV and 8.0 eV, respectively [29].

2.3. Electrostatic energy in the protein

Protein systems contain many ionic groups, which may have an influence upon the ET rate. FD contains Iso as the ET acceptor and the potential ET donors as Trp16, Trp59, Tyr97 and Tyr99. In term of charged residues, FD has 12 Glus, 15 Asps, 2 Lyss, 8 Args amino acid residues plus two negative charges at the FMN phosphate. The ES energy between the Iso anion or donor cation and these ionic groups in the protein is expressed by Eq. (4).

$$E(j) = \sum_{i=1}^{12}\frac{C_j \cdot C_{\mathrm{Glu}}}{\varepsilon_0 R_j(\mathrm{Glu}-i)} + \sum_{i=1}^{15}\frac{C_j \cdot C_{\mathrm{Asp}}}{\varepsilon_0 R_j(\mathrm{Asp}-i)} + \sum_{i=1}^{2}\frac{C_j \cdot C_{\mathrm{Lys}}}{\varepsilon_0 R_j(\mathrm{Lys}-i)} + \sum_{i=1}^{8}\frac{C_j \cdot C_{\mathrm{Arg}}}{\varepsilon_0 R_j(\mathrm{Arg}-i)} + \sum_{i=1}^{2}\frac{C_j \cdot C_{\mathrm{P}}}{\varepsilon_0 R_j(P-i)} \quad (4)$$

The values of $j=0$ for the Iso anion, and $j=1$ for $\mathrm{Trp16}^+$, $j=2$ for $\mathrm{Trp59}^+$, $j=3$ for $\mathrm{Tyr97}^+$ and $j=4$ for $\mathrm{Tyr99}^+$. C_j is charge of the aromatic ionic species j, and is equal to $-e$ for $j=0$ and $+e$ for $j=1$ to 4. Thus, $C_{\mathrm{Glu}}(=-e)$, $C_{\mathrm{Asp}}(=-e)$, $C_{\mathrm{Lys}}(=+e)$, $C_{\mathrm{Arg}}(=+e)$ and $C_{\mathrm{P}}(=-e)$ are the charges of Glu, Asp, Lys, Arg and phosphate anions, respectively. We assumed that these groups are all in an ionic state in solution. The distances between the aromatic ionic species j and the ith Glu ($i=1$–12) are denoted as $R_j(\mathrm{Glu}-i)$, while that between the aromatic ionic species j and the ith Asp ($i=1$–15) are denoted as $R_j(\mathrm{Asp}-i)$, and so on.

ES_j in Eq. (5) was expressed as follows:

$$ES_j = E(0) + E(j) \quad (5)$$

Here j has values from 1 to 4, and represents the jth ET donor as described above.

2.4. Fluorescence decays

The observed fluorescence decay of FD has been reported by Mataga et al. [19], and we used two kind decays as the observed fluorescence decay. The first one is derived from the experimentally observed decay and is evaluated as shown in Eq. (6).

$$F_{\mathrm{obs}}(t) = 0.92\exp\left(\frac{-t}{0.158}\right) + 0.08\exp\left(\frac{-t}{500}\right) \quad (6)$$

where the lifetimes are indicated in unit of ps.

However, the decay was also alternatively evaluated as shown in Eq. (7), where the minor component with a lifetime of greater than 500 ps was neglected, since this was interpreted as being due to free FMN dissociated from the protein [24,25].

$$F_{\mathrm{obs}}(t) = \exp\left(\frac{-t}{0.158}\right) \quad (7)$$

The calculated fluorescence decay is expressed as Eq. (8).

$$F_{\mathrm{calc}}(t) = \left\langle \exp - \left\{\sum_{j=1}^{4} k_{\mathrm{ET}}^{j}(t')\right\} t \right\rangle_{\mathrm{AV}} \quad (8)$$

Fluorescence decays were calculated up to 2 ps with time intervals of 0.002 ps, since the decay was measured in this time range [19]. Note that $\langle\ldots\rangle_{\mathrm{AV}}$ means the averaging procedure of the exponential function in Eq. (8) over t' up to 2 ns with 0.1 ps time intervals. In addition, Eq. (8) assumes that the decay function at every instant of time, t', during the MD time range can be always expressed by the exponential function. The present method is mathematically

equivalent to the one by Henry and Hochstrasser [30], when the time range (2 ns) of MD data is much longer than one (2 ps) of fluorescence data, as described in Supplemental Material.

The unknown ET parameters (ν_0^q, β^q, and R_0^q for Trp and Tyr, G_{Iso}^0 and ε_0) contained in the KM theory were determined so as to obtain the minimum value of χ^2, defined by Eq. (9), by means of a non-linear least squares method, according to the Marquardt algorithm, as previously reported [10–13]. These were then used to obtain the minimum value of χ^2, as defined by Eq. (9).

$$\chi^2 = \frac{1}{N}\sum_{i=1}^{N}\frac{\{F_{calc}(t_i) - F_{obs}(t_i)\}^2}{F_{calc}(t_i)} \quad (9)$$

Here, N denotes number of time intervals of the fluorescence decay, and was 1000. Deviation between the observed and the calculated intensities was expressed by Eq. (10).

$$\text{Deviation}\,(t_i) = \frac{\{F_{calc}(t_i) - F_{obs}(t_i)\}}{\sqrt{F_{calc}(t_i)}} \quad (10)$$

2.5. Quantum chemical calculation

Dipole moments of the Trp59–Iso*–Tyr97 systems, of which configurations were extracted from the MD simulations. MO calculations were performed by a semi-empirical (PM6 method) with the MOPAC2009 software. The keywords, EF (geometrical optimization); PRECISE (accurate calculation); PM6 (semi-empirical Hamiltonians); XYZ (geometry expressed by (x, y, z) coordinates); GEO-OK (neglect check on abnormal access of atoms); EPS (dielectric constant for COSMO solvation energy) and EXCITED (first excited singlet state to be optimized) were used for the calculation (for details of these keywords visit the website: http://openmopac.net/).

The charge densities of Trp59, Iso* and Tyr97 were obtained as the sums of Mulliken charge of the constituent atoms in Trp59, Iso* and Tyr97, respectively. This interaction energy (kcal/mol) of the Trp59–Iso*–Tyr97 system was calculated by Eq. (11).

$$\Delta E = \Delta H_f(\text{Trp59–Iso*–Tyr97}) - \Delta H_f(\text{Trp59}) - \Delta H_f(\text{Iso}*) - \Delta H_f(\text{Tyr97}) \quad (11)$$

In Eq. (11) ΔH_f(Trp59–Iso*–Tyr97), ΔH_f(Trp59), ΔH_f(Iso*) and ΔH_f(Tyr97) were heat of formation of Trp59–Iso*–Tyr97 system, Trp59 system, Iso* system and Tyr97 system, respectively. The heat of formation contains the total electronic energy, the core–core repulsion energy between atoms and the heat of formation of all constituent atoms.

3. Results

3.1. Geometrical factors of FD

The protein structure of FD at the FMN binding site was determined by the method of homology modeling, and is shown in Fig. 1. Time-dependent changes in the center-to-center (R_c) distances in the Iso* and Tyr97, Trp59, Trp16, Tyr99 pairs are shown in Fig. 2, while the changes in the edge-to-edge distances (R_e) are shown in Fig. 3. Of these aromatic amino acids Trp16 is clearly by far the furthest away from Iso, and oscillates the most over time, followed by Tyr99 as determined by both R_c and R_e values. However although both Trp59 and Tyr97 are closer, remain relatively more static over time and are somewhat close in distance from Iso to each other, interestingly they show an inversion between R_c and R_e values. Thus by R_c Tyr97 is the closet residue to Iso, while conversely by R_e it is Trp 59. Fig. 4 shows the time-dependent changes in interplanar angles between Iso and the aromatic amino acids, with the

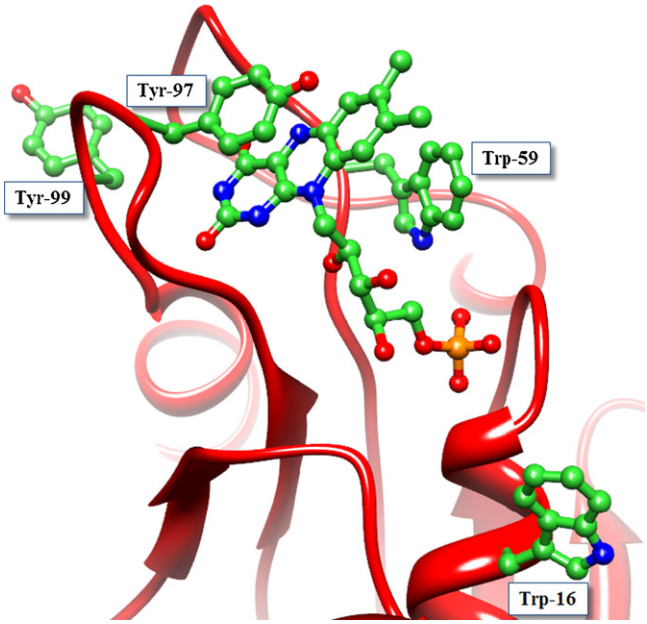

Fig. 1. Structure of FD obtained by a method of homology modeling.

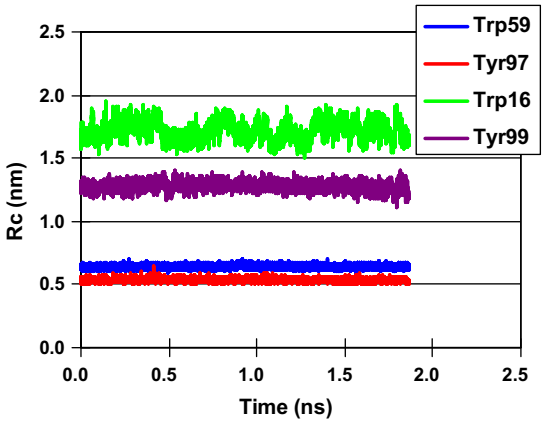

Fig. 2. Center to center distances between Iso and nearby aromatic amino acids in WT. R_c denotes center to center distance. Trp59, Tyr97, Trp16 and Tyr99 indicate the distances between Iso and Trp59, between Iso and Tyr97, between Iso and Trp16, and between Iso and Tyr99.

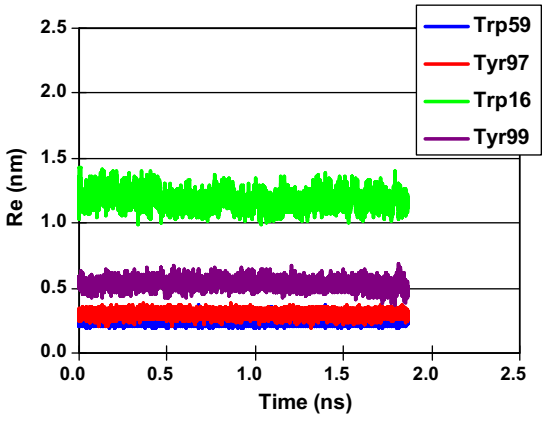

Fig. 3. Edge to edge distances between Iso and nearby aromatic amino acids in WT. R_e denotes edge to edge distance. Trp59, Tyr97, Trp16 and Tyr99 indicate the distances between Iso and Trp59, between Iso and Tyr97, between Iso and Trp16, and between Iso and Tyr99.

Table 1
Physical constants of Iso and aromatic amino acids.[a]

Physical quantity	Iso	Tyr97	Trp59	Trp16	Tyr99
R_c[b] (nm)		0.536 ± 0.0009	0.642 ± 0.0010	1.72 ± 0.0053	1.28 ± 0.0024
Re[c] (nm)		0.301 ± 0.0015	0.247 ± 0.0015	1.18 ± 0.0045	0.533 ± 0.0026
Inter-planar angle (°)		14.0 ± 0.05	-42.8 ± 0.05	-18.0 ± 0.06	23.5 ± 0.07
ES energy[d] (eV)	2.83 ± 0.0006	-2.93 ± 0.0009	-2.85 ± 0.0006	-0.0993 ± 0.0001	-0.118 ± 0.0002
ES[e] (eV)		-0.0942	-0.0172	2.73	2.71
ET rate[f] (ps^{-1})		$(1.26 \pm 0.007) \times 10^{-3}$	7.11 ± 0.015	$(5.33 \pm 0.048) \times 10^{-55}$	$(1.15 \pm 0.033) \times 10^{-50}$

[a] The physical quantities were obtained taking average over MD time (2 ns) at time intervals of 0.1 ps. Mean ± SE was shown.
[b] Center to center distance.
[c] Edge to edge distance.
[d] *ES* energy between Iso anion produced by ET and all ionic amino acids, between Tyr97 cation and all ionic amino acids, between Trp cation and all ionic amino acids, and so on.
[e] *ES* energy given by Eq. (5).
[f] ET rate given by Eq. (1).

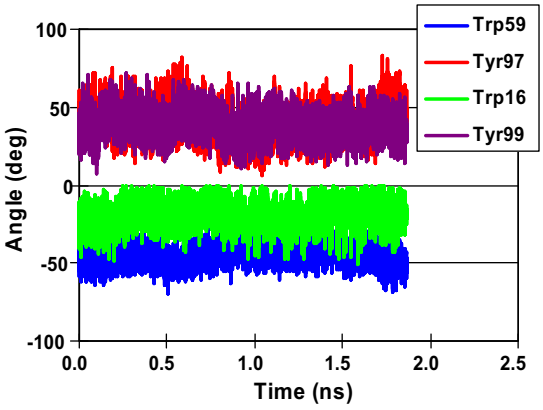

Fig. 4. Inter-planer angles between Iso and nearby aromatic amino acids in WT. Trp59, Tyr97, Trp16 and Tyr99 indicate the distances between Iso and Trp59, between Iso and Tyr97, between Iso and Trp16, and between Iso and Tyr99.

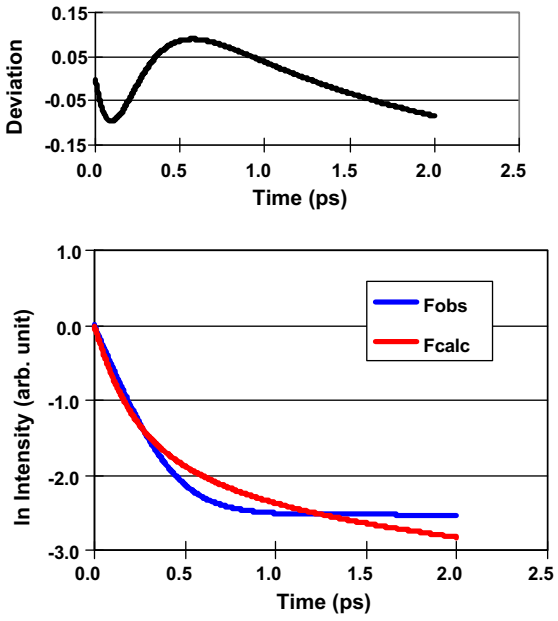

Fig. 5. Fluorescence decays of WT with two lifetime components. The observed decay Fobs is given by Eq. (6). F_{calc} is the calculated decay and obtained with the best-fit ET quantities listed in Table 2. Upper panel is deviation given by Eq. (10) in text. The value of χ^2 was 3.42×10^{-3}.

mean distances listed in Table 1. The mean R_c value between Iso and Tyr97 was 0.54 nm, which was the closest of the aromatic amino acid residues. The other R_c values between Iso and Trp59, Trp16 and Tyr97 were 0.64, 1.72 and 1.3 nm, respectively, while the corresponding values of R_e were 0.301, 0.247, 1.18 and 0.533 nm for Iso to Tyr97, Trp59, Trp16 and Tyr99, respectively. Thus, R_e was shortest in the Iso–Trp59 pair, although the shortest R_c value was between Iso and Tyr97. This discrepancy is because Iso and Tyr97 are almost parallel as seen by the inter-planar angle. Indeed, the inter-planar angles between Iso and the aromatic amino acids were 14°, −43°, −18° and 24° in Tyr97, Trp59, Trp16 and Tyr99, respectively. The R_c between Iso and Tyr97, for instance, was the shortest and they are almost parallel in orientation.

3.2. Fluorescence decays

Fig. 5 shows the observed (F_{obs}) and calculated (F_{calc}) fluorescence decays of the FD. The calculated decay was obtained with the best-fit ET quantities and listed in Table 2. The physical quantities for Trp and Tyr, respectively, were $\nu_0 = 2.06 \times 10^3$ and 5.00×10^2 ps^{-1}, $\beta = 21.9$ and 9.99 nm^{-1} and $R_0 = 0.518$ and 0.694 nm. In addition, $G^0_{Iso} = 7.54$ eV and $\varepsilon_0 = 2.16$. The value of χ^2 was 3.42×10^{-3}. The agreement between the observed and the calculated decays was not good, and the long tail with a fluorescent decay of more than 500 ps lifetime [19] could not be reproduced. Fig. 6 shows fluorescence decays with Eq. (7) as the observed fluorescence dynamics. When the longer lifetime fluorescence decay (500 ps) was assumed to be due to free FMN dissociated from the protein and so ignored, the fluorescence decay could be evaluated with Eq. (7) as the observed fluorescence dynamics (Fig. 6). The physical quantities determined with Eq. (7) for Trp and Tyr, respectively, were $\nu_0 = 3.08 \times 10^3$ and 2.46×10^3 ps^{-1}, $\beta = 55.6$ and 9.64 nm^{-1}, $R_0 = 0.772$ and 0.676 nm, $G^0_{Iso} = 7.67$ eV and $\varepsilon_0 = 5.85$. These parameters were determined by analyzing the fluorescence

Table 2
Physical constants contained in KM theory.[a]

The observed decay	Trp			Tyr			G^0_{Iso} (eV)	ε_0	χ^2
	ν_0 (ps^{-1})	β (nm^{-1})	R_0 (nm)	ν_0 (ps^{-1})	β (nm^{-1})	R_0 (nm)			
Two lifetimes	2056	21.9	0.518	500	9.99	0.694	7.54	2.16	3.42×10^{-3}
Single lifetime[b]	3087	55.6	0.772	2455	9.64	0.676	7.67	5.85	9.55×10^{-5}

[a] Meanings of the physical constants are described in Eq. (1), and bellow.
[b] Data were taken from unpublished work.

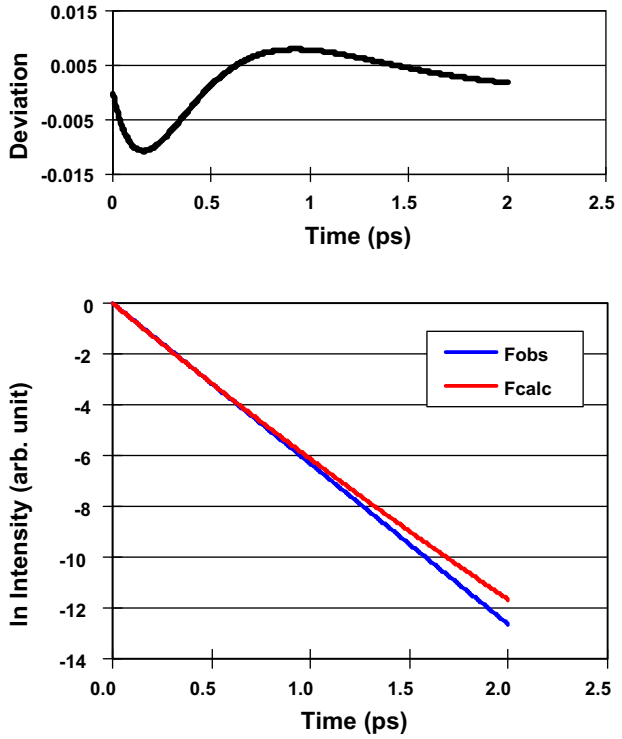

Fig. 6. Fluorescence decays of FD. F_{obs} and F_{calc} denote the observed and calculated fluorescence intensities. Upper panel shows deviation between the observed and the calculated intensities.

decays of the WT, W59F, Y97F and W59F-Y97F double mutation FD's together at once.

3.3. ET rates

Fig. 7 shows representative time-dependent changes in ET rates from Trp59, from Tyr97, from Trp16 and from Tyr99 to Iso*. The mean ET rates are also listed in Table 1. The mean ET rates were 1.26×10^{-3} ps^{-1} from Tyr97, 7.11 ps^{-1} from Trp59, 5.33×10^{-55} ps^{-1} from Trp16, and 1.15×10^{-50} ps^{-1} from Tyr99. It is noted that ET rate was fastest from Trp59, despite that the donor–acceptor distance was shortest between Iso and Tyr97 (see Table 1).

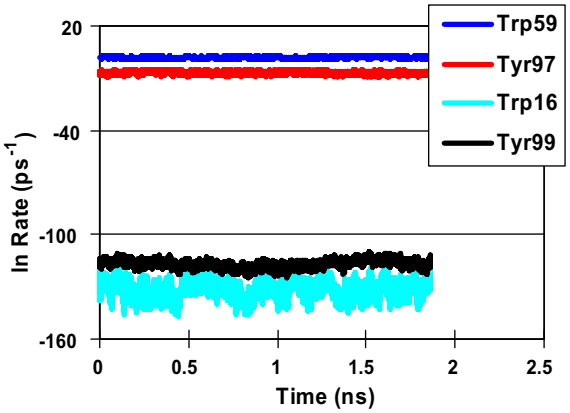

Fig. 7. ET rate from aromatic amino acids to Iso* in FD. Trp59, Tyr97, Trp16 and Tyr99 indicate ET rates from these amino acids to Iso*. ET rate is expressed in unit of ps^{-1}.

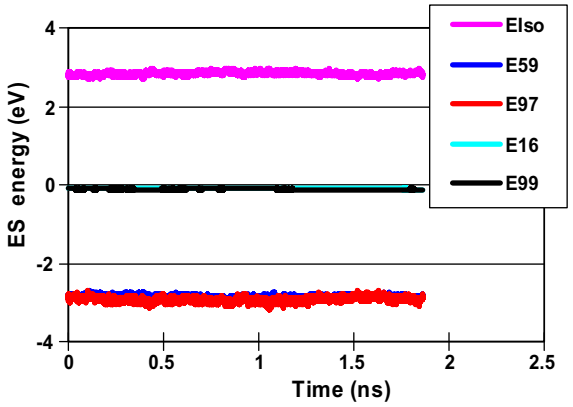

Fig. 8. *ES* energy between ionic species produced by ET and ionic amino acids in WT. Eiso denotes *ES* energy between Iso anion and all ionic amino acids. E59, E97, E16 and E99 indicate electrostatic energy between aromatic cations (Trp59, Tyr97, Trp16 and Tyr99, respectively) and all ionic amino acid residues. $\varepsilon_0 = 5.85$ was used as described in text.

3.4. ES energy

The time-dependent changes in the *ES* energies are shown in Fig. 8. The mean energies were 2.83 eV at Iso anion, −2.93 eV at Tyr97 cation, −2.85 eV at Trp59 cation, −0.099 eV at Trp16 cation, and −0.118 eV at Tyr99 cation (see Table 1). Net *ES* energies given by Eq. (5) are important for the ET rate (see Eq. (1)). The values of net *ES* energies were −0.0942 eV for Tyr97, −0.0172 eV for Trp59, 2.73 eV for Trp16, and 2.71 eV for Tyr99.

3.5. Dipole moment of the Trp59–Iso*–Tyr97 system

Fig. 9 shows a typical dipole moment of the Trp59–Iso*–Tyr97 system, which conformation was obtained from a snapshot of the MD trajectory. The dipole moment was 22.9 D, and its direction was from Iso* to Trp59. The COSMO solvation effect of the electronic states was introduced, using the dielectric constant value of $\varepsilon_0 = 5.85$ (see Table 2). The dipole moment of Iso* alone was 12.4 D, and its direction was in the plane of Iso*. Fig. 10A shows time-dependent change in the dipole moment of Trp59–Iso*–Tyr97 systems. Every snapshot of MD structures at 40 ps time intervals was geometrically optimized. The dipole moment changed with time from 10.4 to 32.3 D. Mean dipole moment was 22.0 D.

3.6. Charge transfer interaction

In the present work the terminology "charge transfer" is used when a non-zero partial charge in any of Trp, Tyr and Iso* is obtained by MO. Iso* must be negatively charged after ET and Trp59/Tyr97 should be positively charged (cationic) because they will loose an electron. Time-dependent changes in the charge densities of

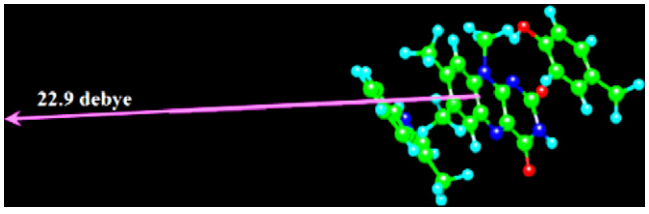

Fig. 9. Dipole moment in the system of Iso*–Tyr97–Trp59 in WT FD. Iso (center) is sandwiched by Trp59 (upper) and Tyr97 (lower). This conformation was obtained by a snapshot of MD structure, where only Iso, Trp59 and Tyr97 were extracted. The direction of the dipole moment was from Iso* to Trp59, which shows part of charge in Trp59 transferred to Iso*, since the direction should be in the Iso plane without charge transfer interaction between Trp59 and Iso*.

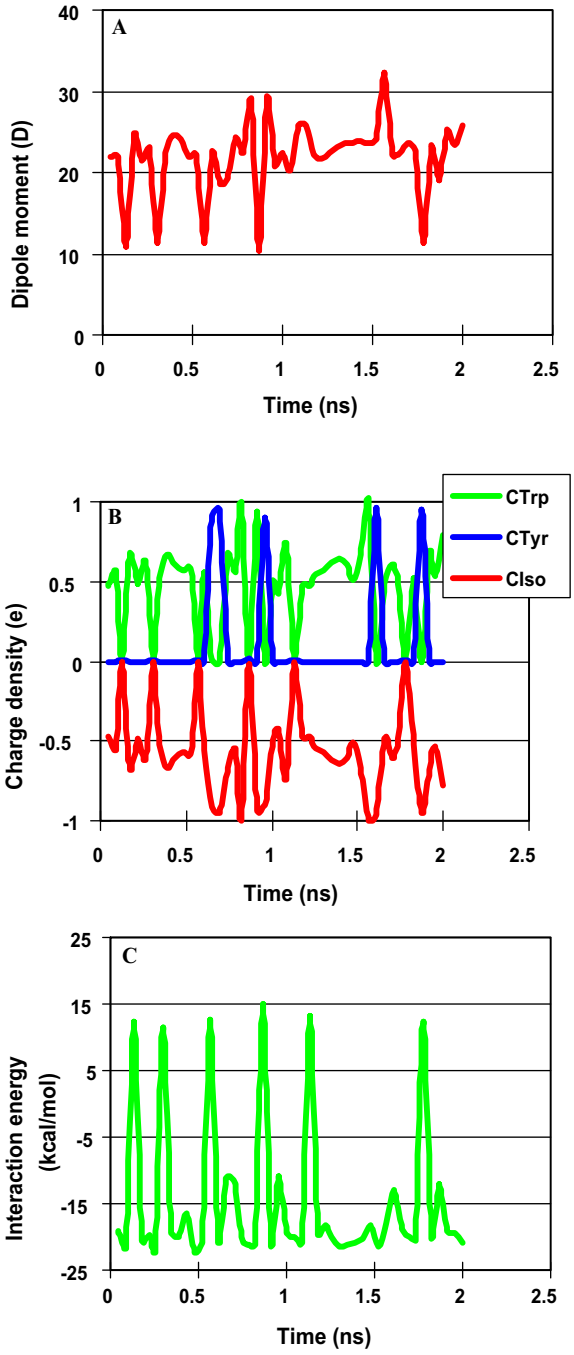

Fig. 10. Charge transfer and interaction energy in the system of Trp59–Iso*–Tyr97 in WT. Dipole moment of Iso* alone was 10.0 D, of which direction was in the plane of Iso. Interaction energy was obtained by Eq. (11).

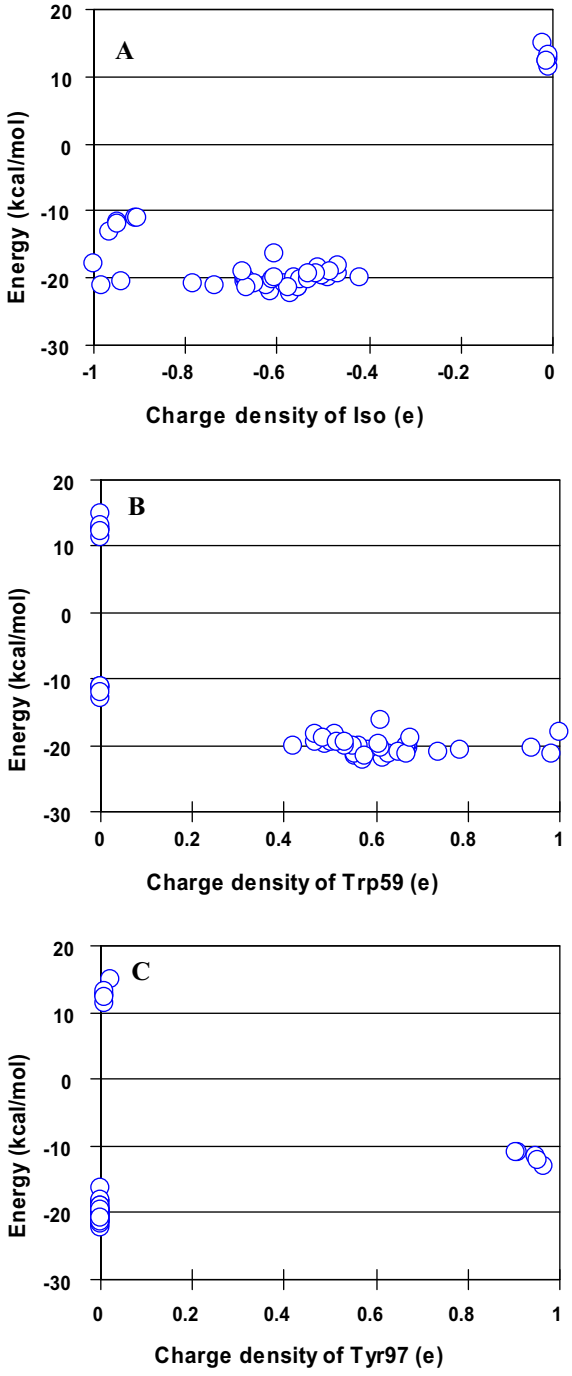

Fig. 11. Correlation between interaction energy and charge densities. (A) Correlations between the interaction energy and the charge density of Iso. (B) Correlation of Trp59, and (C) correlation of Tyr97. Interaction energies were obtained by Eq. (11).

Trp59, Tyr97 and Iso* are shown in Fig. 10B. Charge densities of Iso were always negative or zero. Mean charge density of Iso was −0.568. Charge densities of Trp59 were always positive or zero. Mean charge density of Trp59 was 0.465. Charge densities at Tyr97 were mostly zero, but sometimes displayed positive charge densities, which shows that Tyr97 can be a charge donor to Iso* in the Trp59–Iso*–Tyr97 system. Mean charge density of Tyr97 was 0.103. Fig. 10C shows time-evolution of the interaction energy in Trp59–Iso*–Tyr97 system, which was obtained by Eq. (11). The interaction energy varied from −22 kcal/mol to 15 kcal/mol. Mean interaction energy was −14.9 kcal/mol. In the six snapshots the interaction energies were positive, which implies that the interaction among Trp59, Iso* and Tyr97 was repulsive.

3.7. Correlation

Fig. 11A shows the correlation between the interaction energy and the charge density at Iso*. The interaction energy (absolute value) displayed a tendency to increase with the charge density. It is noted that the interaction energies were positive when the charge densities of Iso* were closed to zero. Correlation between interaction energy and charge density of Trp59 is shown in Fig. 11B. Interaction energy was around −20 kcal/mol, when the amount of charge densities transferred from Trp59 to Iso* were from 0.4 to 1.0. When no charge transfer occurred, the interaction energies were around −12 kcal/mol and around 13 kcal/mol. Even in the negative

energies no charge transfer occurred. Fig. 11C shows correlation between the interaction energy and the charge density of Tyr97. In Tyr97 mostly no charge transfer occurred, but about 0.95 of charge transferred from Tyr97 to Iso* at the energy around −12 kcal/mol. When the interaction energies were positive, the charge transferred little from Tyr97 to Iso*.

4. Discussion

In the present work we have studied the dynamic properties of ET donors and acceptor in FD by MD, and analyzed the ET mechanism using the KM theory and the MD data from the observed fluorescence dynamics. Agreements between the observed and the calculated fluorescence dynamics were very good, when the longer lifetime component of the observed fluorescence dynamics (>500 ps) [19] was neglected. We could not reproduce the observed fluorescence decay with the longer lifetime component by the present method of analysis. Two reasons for this are conceivable. Firstly, the sample was somehow not stable at the fluorescence measurements by an up-conversion instrument system, even though the dissociation constant of FMN is very low (0.38 nM) [17], and thereby the [FMN]/[FD − FMN] is estimated to be 1.23×10^{-3} at [FD − FMN] = 2.5×10^{-4} M for the fluorescence measurements. If we assume that [FMN] and [FD − FMN] are proportional to amplitudes of the shorter lifetime and the longer lifetime, respectively, then [FMN]/[FD − FMN] = 0.087 (9%) [19], which is much larger than one stated above. However, these ratios cannot be compared because of the difference in experimental condition (with and without laser pulsed, [19] and [17], respectively). Therefore, if the sample of WT used for the measurements was not fresh enough, then the intense laser energy could bring the irreversible dissociation of FMN [31]. Secondly, the mathematic model (see Eq. (8)) which assumes that the fluorescence decays exponentially at every instant of MD time, is not valid and so the WT FD consists of two completely different conformers. We support the former interpretation (without the longer lifetime component), because we did not see the predicted conformational change of the second option in the MD snapshots in the time range of 10 ns in WT (see Fig. S1 in Supplemental Material), and we could reasonably analyze four fluorescence decays of WT, W59F, Y97F and W59F-Y97F double mutated FDs (unpublished work).

In the present analysis the ET rate was 7.1 ps^{-1} (lifetime 0.141 ps) from Trp59 to Iso*, and 0.0013 ps^{-1} from Tyr97 in WT. ET rate from Trp59 was ca. 6000 time faster than one from Tyr97, despite that R_c between Iso and Trp59 was longer by 0.1 nm than one between Iso and Tyr97. Experimental average lifetimes were 0.158 ps in WT, 0.808 ps in Y97F and 1.20 ps in W59F [19]. Apparently our result disagrees with the experimental data if we assume that the ET rates of Trp59 and Tyr97 in the WT FD are similar to those of Trp59 in Y97F and Tyr97 in W59F, respectively. However, this assumption is not correct, according to the results of total analyses with the four FD systems together at once (unpublished work). According to this work ET rates were 5.40 ps^{-1} (lifetime 0.185 ps) in Trp59 of Y97F and 3.18 ps^{-1} (lifetime 0.314 ps) in Tyr97 of W59F. ET rate from Trp59 was 1.3 times faster in WT compared to one in Y97F which may be due to *ES* energy changes, and ET rate from Tyr97 was 2400 times slower in WT compared to one in W59F. The reason why ET rates from Trp59 and Tyr97 in WT are different from those in the mutated FDs may be due to the changes in *ES* energy among the proteins.

MO analyses revealed that charge transfer takes place mostly from Trp59 to Iso*, which is in accordance with the ET data. However, charge transfer occasionally occurred from Tyr97 to Iso* (5 times among 46 snapshots), though ET rate from Tyr97 was much slower than one from Trp59. The mean interaction energy obtained by Eq. (11) as evaluated over 46 snapshots at 40 ps time intervals was −15 kcal/mol. The interaction energy (absolute value) was greater as the amount of transferred charge at Iso* increased. The interaction energy, however, was not zero, even though no charge transfer takes place. The phenomena were also observed in FMN-bp system [28]. The occupied molecular orbitals calculated are delocalized between Iso* and Trp59 or Tyr97, even though no charge transfer occurred as in FMN-bp [33]. Fig. 12 shows the electronic delocalization between Iso* and Tyr97 in A and between Iso* and Trp59 in B. This suggests that electrons distribute uniformly between Iso* and Trp59, and so apparently no charge transfer occurred. The electronic delocalization may yield non-zero interaction energy among the chromophores.

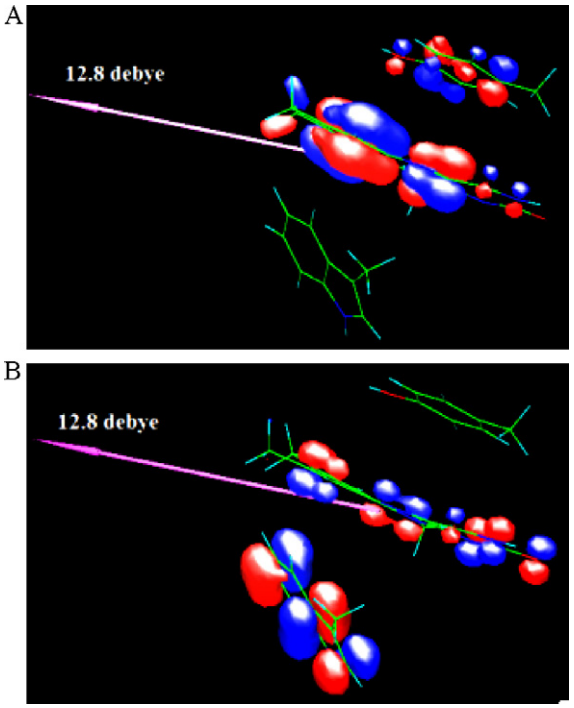

Fig. 12. Electronic delocalization of molecular orbitals in the configuration without appreciable charge transfer. Optimized configuration at 360 ps had low dipole moment and apparently no charge transfer took place. Panels (A) and (B) shows electronic delocalization of molecular orbitals No. 91 and 86, respectively. Orbital No. of HOMO was 94. The electronic delocalization among the three chromophores may yields the non-zero interaction energy.

It is important to consider which factors are influential upon ET rate. Effect of variation in ν_0 on ET rate is considered to be not much compared to the other factors. β and R_0 may be influential factors on ET rate when R_j is longer than R_0 (non-adiabatic process). It is not unreasonable that factors contained in $-\{\Delta G_q^0 - e^2/\varepsilon_0 R_j + \lambda_S^{qj} + ES_j\}^2/4\lambda_S^{qj}k_BT$ in exponential function (see Eq. (1)) are important. R_j is influential through λ_S^{qj} and $-e^2/\varepsilon_0 R_j$. Effect of λ_S^{qj} variation on ET rate may be compensated by λ_S^{qj} in the denominator. Accordingly, $\Delta G_q^0 + ES_j$ may be most important factors. ES_j varies quite a lot with time because it directly depends on the structural dynamics of the protein, while ΔG_q^0 keeps constant. Recently the effect of change in one charge was reported on ultrafast fluorescence dynamics and ET rates from Trp and/or Tyr to Iso* in FMN-bp [32].

Relationship between ET process and electron transfer process in dark is worthy to discuss. The donor–acceptor distance dependence of λ_S^{qj} and $-e^2/\varepsilon_0 R_j$ are common in the both processes except for the distance. *ES* energy of Iso anion and other ionic amino acids is also common between the both electron transfer processes. Many

of flavoproteins involve in electron transfer processes in dark. ET analyses of the flavoproteins could also help to understand the electron transfer in the ground state of Iso.

Acknowledgments

This work was supported by The Royal Golden Jubilee Ph.D. Program (3.C.CU/50/S.1) and by the National Center of Excellence for Petroleum, Petrochemicals and Advanced Materials (NCE-PPAM). Thanks are also given to Computational Chemistry Unit Cell, Chulalongkorn University, and the National Electronics and Computer Technology Center (NECTEC), for computing facilities.

Appendix A. Supplementary data

Supplementary data associated with this article can be found, in the online version, at doi:10.1016/j.jphotochem.2010.11.001.

References

[1] T. Nishino, R. Miura, M. Tanokura, K. Fukui, Flavins and Flavoproteins 2005, Smallworld Publishing Co., Tokyo, 2005.
[2] S. Masuda, C.E. Bauer, Cell 110 (2002) 613–623.
[3] M. Gauden, J.S. Grinstead, W. Laan, I.H.M. van Stokkum, M. Avila-Perez, K.C. Toh, R. Boelens, R. Kaptein, R. van Grondelle, K.J. Hellingwerf, J.T.M. Kennis, Biochemistry 46 (2007) 7405–7415.
[4] A. Kita, K. Okajima, Y. Morimoto, M. Ikeuchi, K. Miki, J. Mol. Biol. 349 (2005) 1–9.
[5] A. Möglich, X. Yang, R.A. Ayers, K. Moffat, Annu. Rev. Plant. Biol. 61 (2010) 21–47.
[6] R.A. Marcus, J. Chem. Phys. 24 (1956) 979–989.
[7] C.C. Moser, J.M. Keske, K. Warncke, R.S. Farid, P.L. Dutton, Nature 355 (1992) 796–802.
[8] M. Bixon, J. Jortner, J. Phys. Chem. 95 (1991) 1941–1944.
[9] T. Kakitani, N. Mataga, J. Phys. Chem. 89 (1985) 8–10.
[10] N. Nunthaboot, F. Tanaka, S. Kokpol, H. Chosrowjan, S. Taniguchi, N. Mataga, J. Photochem. Photobiol. A: Chem. 201 (2009) 191–196.
[11] N. Nunthaboot, F. Tanaka, S. Kokpol, H. Chosrowjan, S. Taniguchi, N. Mataga, J. Phys. Chem. B 112 (2008) 13121–13127.
[12] N. Nunthaboot, F. Tanaka, S. Kokpol, J. Photochem. Photobiol. A: Chem. 207 (2009) 274–281.
[13] N. Nunthaboot, F. Tanaka, S. Kokpol, J. Photochem. Photobiol. A: Chem. 209 (2010) 79–87.
[14] M.L. Ludwig, C.L. Luschinsky, Structure and redox properties of clostridial flavodoxin, in: F. Müller (Ed.), Chemistry and Biochemistry of Flavoenzymes, CRC Press, Florida, 1992, pp. 427–466.
[15] S.G. Mayhew, G. Tollin, General properties of flavodoxins, in: F. Müller (Ed.), Chemistry and Biochemistry of Flavoenzymes, CRC Press, Florida, 1992, pp. 386–426.
[16] S.G. Mayhew, D.P. O'Connell, P.A. O'Farrell, G.N. Yalloway, S.M. Geoghegan, Biochem. Soc. Trans. 24 (1996) 122–127.
[17] M. Kitamura, T. Sagara, M. Taniguchi, M. Ashida, K. Ezoe, K. Kohno, S. Kojima, K. Ozawa, H. Akutsu, I. Kumagai, T. Nakaya, J. Biochem. 123 (1998) 891–898.
[18] K.D. Watenpaugh, L.C. Sieker, L.H. Jensen, Proc. Natl. Acad. Sci. U.S.A. 70 (1973) 3857–3860.
[19] N. Mataga, H. Chosrowjan, S. Taniguchi, F. Tanaka, N. Kido, M. Kitamura, J. Phys. Chem. B 106 (2002) 8917–8920.
[20] A. Karen, N. Ikeda, N. Mataga, F. Tanaka, Photochem. Photobiol. 37 (1983) 495–502.
[21] A. Karen, M.T. Sawada, F. Tanaka, N. Mataga, Photochem. Photobiol. 45 (1987) 49–54.
[22] D.P. Zhong, A.H. Zewail, Proc. Natl. Acad. Sci. U.S.A. 98 (2001) 11867–11872.
[23] J. Pan, M. Byrdin, C. Aubert, A.P.M. Eker, K. Brettel, M.H. Vos, J. Phys. Chem. B 108 (2004) 10160–10167.
[24] F. Tanaka, R. Rujkorakarn, H. Chosrowjan, S. Taniguchi, N. Mataga, Chem. Phys. 348 (2008) 237–241.
[25] F. Tanaka, H. Chosrowjan, S. Taniguchi, N. Mataga, K. Sato, Y. Nishina, K. Shiga, J. Phys. Chem. B 111 (2007) 5694–5699.
[26] M.A. Marti-Renom, A.C. Stuart, A. Fiser, R. Sanchez, F. Melo, A. Sali, Annu. Rev. Biophys. Biomol. Struct. 29 (2000) 291–325.
[27] D.A. Case, T.A. Darden, T.E. Cheatham III, C.L. Simmerling, J. Wang, R.E. Duke, R. Luo, M. Crowley, R.C. Walker, W. Zhang, K.M. Merz, B. Wang, S. Hayik, A. Roitberg, G. Seabra, I. Kolossváry, K.F. Wong, F. Paesani, J. Vanicek, X. Wu, S.R. Brozell, T. Steinbrecher, H. Gohlke, L. Yang, C. Tan, J. Mongan, V. Hornak, G. Cui, H.D. Mathews, M.G. Seetin, C. Sagui, V. Babin, P.A. Kollman, AMBER10, University of California, San Francisco, 2008.
[28] N. Nunthaboot, F. Tanaka, S. Kokpol, H. Chosrowjan, S. Taniguchi, N. Mataga, J. Phys. Chem. B 112 (2008) 15837–15843.
[29] V. Vorsa, T. Kono, K.F. Willey, N. Winograd, J. Phys. Chem. B 103 (1999) 7889–7895.
[30] E.R. Henry, R.M. Hochstrasser, Proc. Natl. Acad. Sci. U.S.A. 84 (1987) 6142–6146.
[31] P.A.W. van den Berg, J. Widengren, M.A. Hink, R. Rigler, A.J.W.G. Visser, Spectrochim. Acta A 57 (2001) 2135–2144.
[32] H. Chosrowjan, S. Taniguchi, N. Mataga, T. Nakanishi, Y. Haruyama, S. Sato, M. Kitamura, F. Tanaka, J. Phys. Chem. B 114 (2010) 6175–6182.
[33] N. Nunthaboot, F. Tanaka, Pure and Applied Chemistry International Conference 2009, Proceedings, 2009, pp. 495–498.